

Dynamics of Turbulent Ignition in Lean Premixed Methane/Air Gases

S. S. Shy*, W. D. Shih, C. C. Liu, C. M. Huang

Institute of Energy Technology, Department of Mechanical Engineering, National Central University, Jhong-li City, Tau-yuan 32001, Taiwan

1 Introduction

Ignition is the beginning of combustion, which is an elegant way to understand turbulent premixed combustion if flame initiation, kernel formation and its subsequent flame propagation in a combustible mixture at a controllable turbulence environment can be quantitatively measured. As known for a long time, there are different modes of turbulent combustion that may influence all key features of premixed turbulent flames [1], such as “turbulent-flamelet” and “turbulent-distributed” regimes. Traditionally, these two regimes are separated by a $Ka = 1$ line for high Reynolds number turbulent flows [2], where Ka is the turbulent Karlovitz number commonly-defined as $Ka = (u'/S_L)^2 (Re_T)^{-0.5}$ and $Re_T = u'L/\nu$. Here u' , L , ν , and S_L are respectively the characteristic turbulent intensity, the integral length scale of turbulence, the kinematic viscosity, and the laminar burning velocity. This traditional criterion for the transition of combustion modes from flamelet to distributed when $Ka > 1$ has recently been modified by Peters [1] based on a scaling description of the size of the reaction zone. Peters argued that flame broadening by turbulence in the “thin reaction zone” regime occurs only in the preheated zone without much influencing the reaction rate and this thin reaction zone regime before transforming into the “broken reaction zone” regime could sustain for $Ka \gg 1$. Two important questions arise. Can one prove experimentally the existence of the distributed-combustion regime or the thin/broken reaction zones? What is the correct criterion for the transition from flamelet to distributed regimes? Hence, this note addresses these two questions.

When lean premixed turbulent combustion is considered, accurate MIE data are essential for optimization of ignition systems [2,3]. MIE is also an important property for safety standards as well as for the fundamental understanding of the ignition process of combustible mixtures [3-4]. Furthermore, Sánchez, Liñán and their co-workers [5] in a theoretical study pointed out that MIE should be proportional to the volume of the reaction zone, δ^3 , where δ is the reaction zone thickness which may be equivalent to the size of the spark-kernel at least in the beginning of combustion. The higher the ignition energy is, the larger the size of the spark-kernel is. Very recently, Shy and his co-workers [6] showed that measurements of MIE in intense isotropic turbulence without mean velocities can provide an excellent opportunity to scrutinize different combustion modes and thus evaluate the new regime diagram of premixed turbulent combustion proposed by Peters [1]. In [6], only one complete set of MIE data for lean premixed turbulent methane combustion at $\phi = 0.6$ over a wide range of u'/S_L was presented. Therefore, this work aims to investigate the effect of ϕ on MIE. Does the transition on MIE exist at a higher value of ϕ ($= 0.7$)? If so, what is the criterion of the MIE transition at $\phi = 0.7$? Is it the same or different to that of previous data at $\phi = 0.6$ [6]? We will address these questions. Furthermore, flame initiation, kernel formation and its subsequent flame propagation at various turbulent intensities from moderate to very intense are described, and the corresponding turbulent flame speeds are estimated and discussed for the first time.

2 Experimental

Experiments are conducted in a symmetric cruciform burner, consisting of a large horizontal vessel and a vertical vessel, as schematically shown on Fig. 1. In the horizontal cylindrical vessel, two identical fans and perforated plates

*Correspondence to : sshv@ncu.edu.tw

of 36% solidity are installed at both ends. Each of the two fans is independently driven by a 10-HP DC motor and synchronized to the same speed, of which a maximum fan frequency of 172 Hz can be achieved, for either co-rotation or counter-rotation, when the water cooling system is applied to both shafts. In the core region between the two perforated plates, a uniform near-isotropic turbulence region, roughly $15 \times 15 \times 15 \text{ cm}^3$ in volume, can be generated having intense turbulent intensities up to 8 m/s when the two fans are counter-rotating. In it all energy spectra in three directions have $-5/3$ decaying slopes revealing that this flow is a true 3D fully-developed turbulence of a wide range of characteristic scales [7].

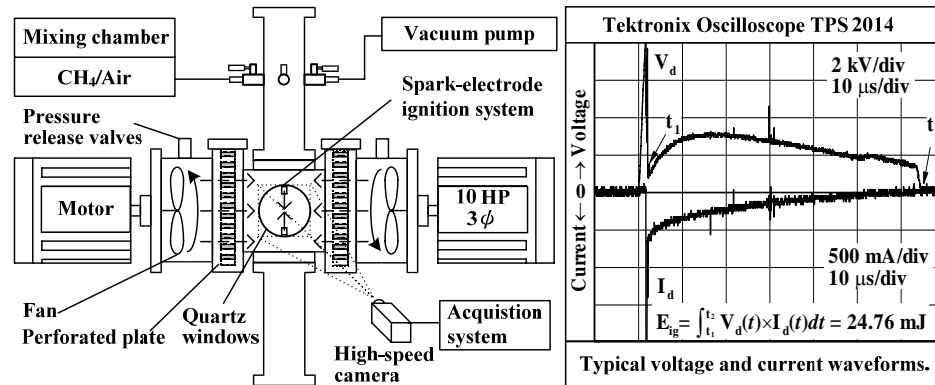


Fig. 1. The fan-stirred cruciform burner with an energy-adjustable spark-electrode ignition system. Typical voltage and current waveforms obtained during an ignition experiment are shown on the right.

Previous studies by Kono and his co-workers [e.g., 3] as well as Ziegler et al. [8] have demonstrated that the ignition energy of spark discharge depends upon gas density and species, electrode material, size and geometry, current, gap width, and type of discharge. For simplicity, the present work applies a commercial high-power pulse generator to control and vary discharge energies of a stainless-steel spark-electrode with very sharp needle ends separated by a fixed gap width of about 2.6 mm. This gap width gives the smallest MIE for lean methane/air mixtures at $\phi=0.6$ and 0.7 using the present stainless-steel spark-electrode (not shown). The spark-electrode ignites lean methane/air mixtures in the central position of the fan-stirred cruciform burner. The high-power spark-discharging system is capable of discharging a high voltage up to 20 kV with selectable pulse durations from 0.05 μs to 3 ms. We apply one shot mode of discharging with a fixed pulse duration of 100 μs for all experiments. A variety of resistances from 0 to 50 k Ω are used to vary spark ignition energies from 0 to about 71 mJ. The right part of Fig. 1 shows typical recording traces of voltage and current waveforms, measured by a Tektronix high-voltage probe and a Pearson current monitor. The discharging spark occurs soon after the onset of initial high voltage output to produce the concurrent voltage (V_d) and current (I_d) waveforms. The value of ignition energy can be thus obtained by integration of the product of $V_d I_d$ from time t_1 to t_2 , as shown on the right of Fig. 1. Observations of ignition spark, flame kernel development and subsequent propagation of a near-spherical flame front (only when the two fans are counter-rotating) are recorded by a high-speed, high resolution CMOS digital camera with 5000 frames/s and 512 \times 512 pixel resolution. Before a run, lean methane/air mixtures are well-mixed in a separate mixing chamber and then fill these premixtures into the evacuated chamber at 1 atm. A run begins by igniting the mixture under the quiescent condition or at various turbulent intensities.

Concerning the definition of MIE, we use the same definition as that used by previous studies [e.g., 2,3,6,8] of which MIE is the ignition energy of 50% ignitability at a given flow condition and a fixed ϕ . A range of ignition energy data between 100% and 0% ignitability is first captured and then continuously narrowed down to identify the ignition energy of 50% ignitability, $E_{ig(50\%)} (\equiv \text{MIE})$. In this study, each data point of $E_{ig(50\%)}$ for a given mixture at a fixed flow condition is determined by more than 30 repeated runs to ensure the accuracy of statistics.

3 Results and Discussion

Figures 2(a)~2(e) display instantaneous sequential images of spark-ignition, flame kernel formation and its subsequent flame propagation for lean methane/air mixtures at $\phi=0.7$ in three different combustion modes. (1) The laminar mode where $u'/S_L=0$ and/or $Ka=0$ (Fig. 2a), (2) the turbulent-flamelet mode with moderate u'/S_L and/or $Ka<1$ (Figs. 2b~2d), and (3) the turbulent-distributed mode where $u'/S_L=32.6$ and/or $Ka\sim 10 \gg 1$ (Fig. 2e), respectively.

In the quiescent condition without fan-rotated, the flame kernel development and subsequent propagation of flame fronts remain quasi-symmetric with respect to the electrode having approximately spherical geometry during all periods of time studied. When only one fan rotates with the other fan stationary, just as presented on Figs. 2b, flame propagation is much faster toward the rotating fan, demonstrating a strong influence of turbulence on flame propagation. This influence can be even obviously seen for the case when the two fans are co-rotating, of which flame kernel development and subsequent propagation of flame fronts become a long cylindrical shape (Fig. 2c). Only when the two fans are counter-rotating, the flow can have a very high degree of isotropy, of which flame kernel development and subsequent propagation of flame fronts are near-spherical (Figs. 2d; the turbulent-flamelet mode) where flames are highly corrugated and cellular since the Lewis number is less than unity. It is found that flame kernels from initiation to development up to 10 ms are essentially the same for both turbulent-flamelet and laminar modes even when values of u'/S_L are as much as 24 corresponding to $Ka \sim 6$. Similar results were also reported by [3,6]. For very intense turbulence level where $u'/S_L = 32.6$ and $Ka \gg 1$ (Fig. 2e), significantly higher ignition energies are required to ignite the same methane/air mixtures at $\phi = 0.7$. The development of turbulent flame kernel takes only several milliseconds after the spark-discharge, and the flame kernel may occur at random positions slightly outside the electrode gap (see the image at 4 ms on Fig. 2e). Furthermore, from images at 4 ms up to 10 ms on Fig. 2e, distributed propagation flames with filiform edges (highly dispersive and fragmental) are observed, which are quite different to turbulent-flamelet flames of clear-cut structures.

Figure 3 shows a complete data set of MIE as a function of u'/S_L ranging from 0 to about 35 for lean turbulent methane combustion at $\phi=0.7$ (black circles). Also plotted are the MIE curve at $\phi=0.6$ (white circles) for comparison. Both MIE values at the quiescent condition ($u'/S_L=0$) are marked on the ordinate with white and black triangular symbols, which are 2.14 mJ and 0.727 mJ for $\phi=0.6$ and 0.7, respectively. All MIE data at $\phi=0.7$ are much smaller than that of $\phi=0.6$ at any fixed values of u'/S_L . A transition on MIE for lean turbulent methane combustion at $\phi=0.7$ is found to occur around $u'/S_L > 25$ corresponding to $Ka > 7$, similar to that found in [6] for $\phi=0.6$. Before the transition, values of MIE at $\phi=0.7$ only increase gradually from about 0.73 to 1.7 mJ when values of u'/S_L increase from 0 to about 20, at which $E_{ig(50\%)} \sim (u'/S_L)^{0.3}$. Across the transition, values of MIE at $\phi=0.7$ increase abruptly from about 4 mJ to 42 mJ when values of u'/S_L only increase from about 25 to 32, at which $E_{ig(50\%)} \sim (u'/S_L)^7$. The log-log plot of $E_{ig(50\%)}$ versus u'/S_L clearly shows a drastic increase of the power constant jumping from 0.3 to 7, as shown on Fig. 3. However, more experiments need to be conducted near the transitional region between $u'/S_L \sim 20$ and $u'/S_L \sim 24$ for clarifying the precise position of the transition.

By comparing these averaged radii of expanding flame fronts in both laminar and turbulent-flamelet modes at the same instants (Figs. 2a and 2d for counter-rotation cases), it can be clearly seen that turbulence can increase flame propagation speeds to a value much higher than laminar flames can achieve. Flame propagation speeds are estimated by the slopes of these averaged radii of expanding flame fronts as a function of time. Due to the space limit, more discussion will be given in the near future.

References

- [1] Peters N. (2000). *Turbulent Combustion*, Cambridge University Press, Cambridge
- [2] Maly R. and Vogel M. (1979). Initiation and Propagation of Flame Fronts in Lean CH₄-Air Mixtures by the Three Modes of the Ignition Spark, *Proc. Combust. Inst.* **17**: 821
- [3] Ishii K., Aoki O., Ujiie Y., Kono, M. (1992). Investigation of Ignition by Composite Sparks under High Turbulence Intensity Conditions, *Proc. Combust. Inst.* **24**: 1793
- [4] Fisher F. A. (2000). *Some Notes on Sparks and Ignition of Fuel*, Tech. Memo. NASA/TM-2000-210077, Washington
- [5] Kurdyumov V., Blasco J., Sánchez A. L., Lián A. (2004). On the Calculation of the Minimum Ignition Energy, *Combust. Flame* **136**: 394
- [6] Huang C. C., Shy S. S., Liu C. C., and Yan Y. Y. (2007). A Transition on Minimum Ignition Energy for Lean Turbulent Methane Combustion in Flamelet and Distributed Regimes, *Proc. Combust. Inst.* **31**: 1401
- [7] Shy S. S., Lin W. J., Wei, J. C. (2000). An Experimental Correlation of Turbulent Burning Velocities for Premixed Turbulent Methane-Air Combustion. *Proc. Roy. Soc. London A* **456**: 1997; Yang T. S., Shy S. S. (2005). Two-Way Interaction between Solid Particles and Homogeneous Air Turbulence: Particle Settling Rate and Turbulence Modification Measurements. *J. Fluid Mech.* **526**: 171
- [8] Ziegler G. F. W., Wagner E. P. and Maly, R. R. (1984). Ignition of Lean Methane-Air Mixtures by High Pressure Glow and Arc Discharges, *Proc. Combust. Inst.* **20**: 1817

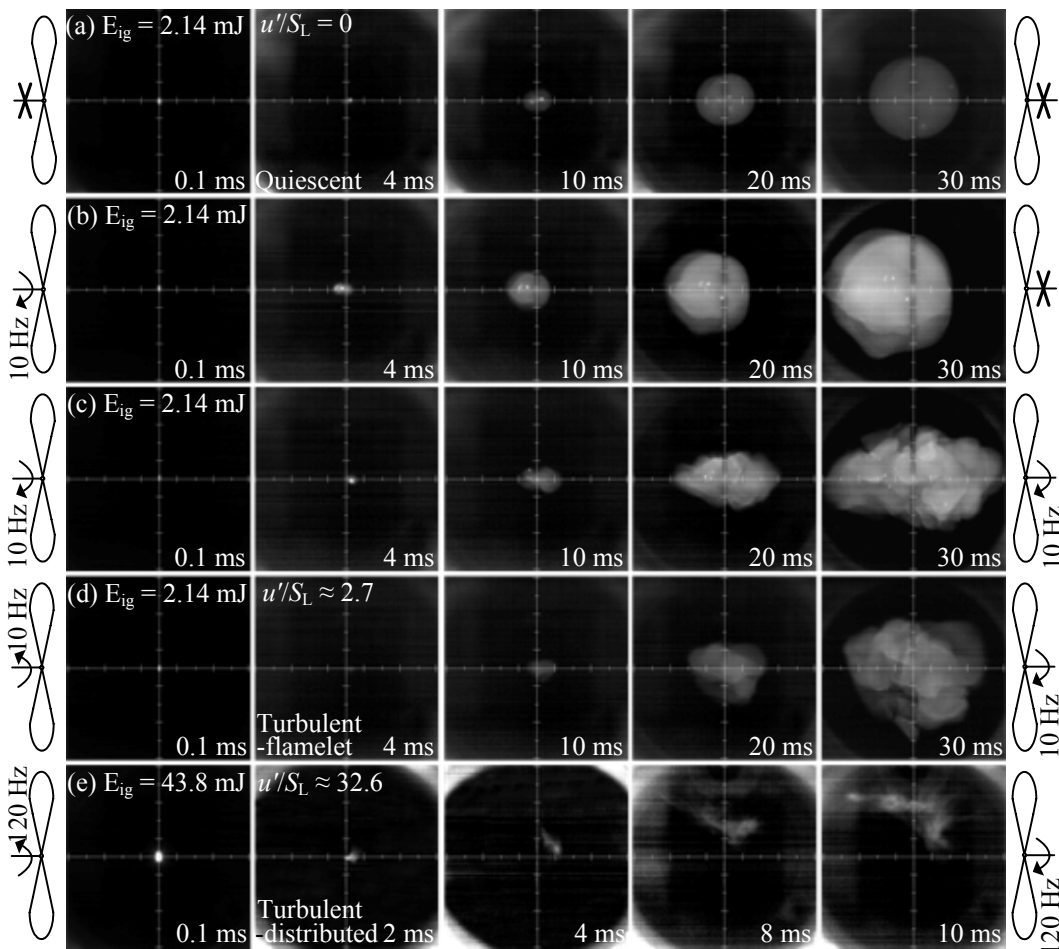


Fig. 2. Sequent instantaneous images showing spark-ignition and flame propagation of lean premixed methane/air mixtures at $\phi=0.7$ under (a) laminar and (b-e) various turbulent conditions, as indicated by the cross symbol (without fan rotation) and directionally rotational arrows with different fan frequencies.

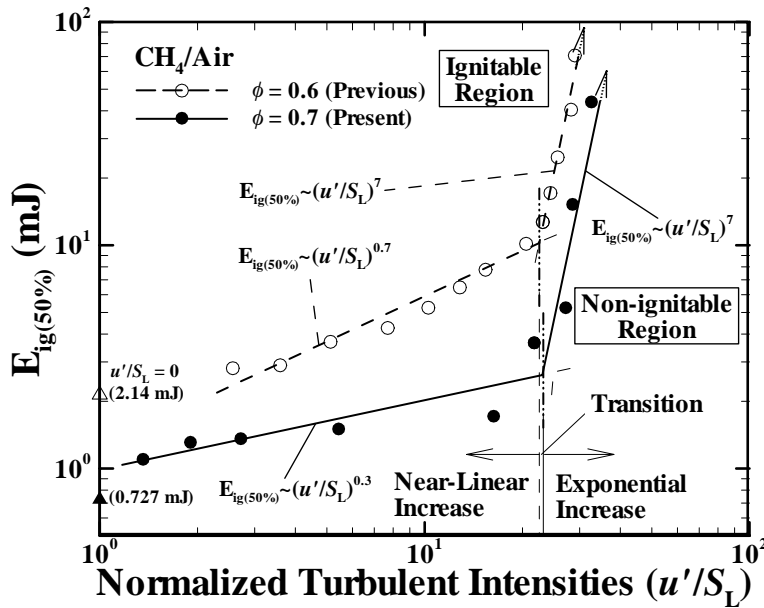


Fig. 3. Turbulent minimum ignition energies as a function of turbulent intensities at $\phi = 0.7$ (present data) and $\phi = 0.6$ (previous data).